

of electron emission does not seem to be as important at 7.3 keV electron energy as compared to lower energies where our experimental data points are lower than the values computed from Ref. 15 (not shown in Fig. 2).

Summarizing, we say that our experiments verified for the first time that depth-selective ^{57}Fe conversion-electron Mössbauer spectra can be obtained with a spatial resolution which is in agreement with existing theoretical predictions.

We are indebted to Dr. J. Lauer for preparing the thin-film specimen. Financial support by the Deutsche Forschungsgemeinschaft is gratefully acknowledged.

^(a)On leave from the Institute for Chemical Research, Kyoto University, Uji, Japan.

¹See, e.g., F. E. Wagner, J. Phys. (Paris), Colloq. **37**, C6-673 (1976).

²Zw. Bonchev, A. Jordanov, and A. Minkova, Nucl. Instrum. Methods **70**, 36 (1969).

³R. A. Krakowski and R. B. Miller, Nucl. Instrum. Methods **100**, 93 (1972).

⁴M. Bäverstam, T. Ekdahl, Ch. Bohm, B. Ringström, V. Stefansson, and D. Liljequist, Nucl. Instrum. Methods **115**, 373 (1974).

⁵M. Bäverstam, T. Ekdahl, C. Bohm, D. Liljequist, and B. Ringström, Nucl. Instrum. Methods **118**, 313

(1974).

⁶N. Benczer-Koller and B. Kolk, in *Workshop on New Directions in Mossbauer Spectroscopy—1977*, edited by Gilbert J. Perlow, AIP Conference Proceedings No. 38 (American Institute of Physics, New York, 1977), Vol. 38, p. 107.

⁷M. R. Polcari, J. Parellada, K. Burin, and G. M. Rothberg, Inst. Phys. Conf. Ser. **39**, 584 (1978).

⁸M. Bäverstam, B. Bodlund-Ringström, C. Bohm, T. Ekdahl, and D. Liljequist, Nucl. Instrum. Methods **154**, 401 (1978).

⁹T. Toriyama, K. Saneyoshi, and K. Hisatake, J. Phys. (Paris), Colloq. **40**, C2-14 (1979).

¹⁰M. Domke, B. Kyvelos, and G. Kaindl, in Proceedings of the Fifth International Conference on Hyperfine Interaction, West Berlin, Federal Republic of Germany, 21–25 July, 1980 (to be published).

¹¹T. Shigematsu, H.-D. Pfannes, and W. Keune, in Applications of Mössbauer Spectroscopy, edited by Richard L. Cohen (Academic Press, New York, to be published).

¹²H. Ibach, in *Electron Spectroscopy for Surface Analysis*, edited by H. Ibach (Springer, Berlin, 1977), p. 1.

¹³M. Petrera, U. Gonser, U. Hasmann, W. Keune, and J. Lauer, J. Phys. (Paris), Colloq. **37**, C6-295 (1976).

¹⁴D. Liljequist, T. Ekdahl, and M. Bäverstam, Nucl. Instrum. Methods **155**, 529 (1979).

¹⁵D. Liljequist and B. Bodlund-Ringström, Nucl. Instrum. Methods **160**, 131 (1979).

¹⁶A. Proykova, Nucl. Instrum. Methods **160**, 321 (1979).

Solitons in Polyacetylene: Effects of Dilute Doping on Optical Absorption Spectra

N. Suzuki,^(a) M. Ozaki,^(b) S. Etemad, A. J. Heeger, and A. G. MacDiarmid

Laboratory for Research on the Structure of Matter, University of Pennsylvania, Philadelphia, Pennsylvania 19104

(Received 9 June 1980)

A joint theoretical and experimental study of the effects of dilute doping on the optical absorption spectra of *trans*-polyacetylene, *trans*-(CH)_x, is presented. It is shown that the optical transition between a band state and the soliton level is considerably enhanced. However, the existence of a soliton kink strongly suppresses the interband transition. The agreement between theory and experiment supports the applicability of the soliton model to *trans*-(CH)_x.

PACS numbers: 78.50.Ge, 61.40.Km

Interest in the study of the physics of polyacetylene, (CH)_x, has focused on the proposal^{1,2} that neutral and charged amplitude solitons dominate the magnetic, electrical, and optical properties. The soliton picture has received increasing experimental support through analysis of the magnetic,³⁻⁶ infrared,^{7,8} transport,^{9,10} and phototransport¹¹ properties of lightly doped samples. Tomkiewicz *et al.*¹² have asserted, however, that the

soliton domain walls do not exist and that the properties of doped (CH)_x are determined by an inhomogeneous mixture of metallic islands in undoped (CH)_x.

In this paper we examine the effects of soliton doping on the optical absorption spectra. Calculations of the absorption coefficient (α) show that a soliton kink on a chain suppresses the interband transition, whereas transitions involving the

soliton level are found to have a significantly enhanced absorption cross section. The results are in agreement with the experimental absorption spectra obtained from *trans*-(CH)_x lightly doped with AsF₅.

Takayama, Lin-Liu, and Maki¹³ considered the continuum limit of the linear-chain model introduced by Su, Schrieffer, and Heeger¹ to describe (CH)_x. Their analytical results are in agreement with the numerical results of Su, Schrieffer, and Heeger and allow explicit calculation of wave functions and matrix elements. The effective Hamiltonian¹³ for the continuum model is

$$H = -iv_F \sigma_3 \partial / \partial x + \Delta(x) \sigma_1 \quad (1)$$

with the Fermi velocity $v_F = 2t_0 a$. The σ 's are Pauli matrices, a and t_0 are the lattice constant and nearest-neighbor transfer integral, respectively, of the uniform (undimerized) chain, and $\Delta(x)$ is the order parameter describing the dimerization pattern. To calculate $\alpha(\omega)$, we need matrix elements of the momentum operator, which can be expressed in the continuum model in the form $p_x = 2M_x i \sigma_3$ where $M_x \equiv -i\hbar \int \varphi(x, y, z) \times \partial \varphi(x - a, y, z) / \partial x dx dy dz$ and φ is the atomic $\pi(p_x)$ orbital of the carbon atoms.¹

For a perfect dimerized chain [$\Delta(x) = \Delta_0$], the interband absorption coefficient (per carbon atom), for transitions from valence band (VB) to conduction band (CB), is

$$\alpha_i(\omega) = A f_i(\omega), \quad (2)$$

$$f_i(\omega) = (E_g / \hbar \omega)^2 E_g / [(\hbar \omega)^2 - E_g^2]^{1/2}, \quad (3)$$

where $A \equiv (16\pi \hbar e^2 |M_x|^2) / m^2 n c W E_g$, $E_g = 2\Delta_0$, W

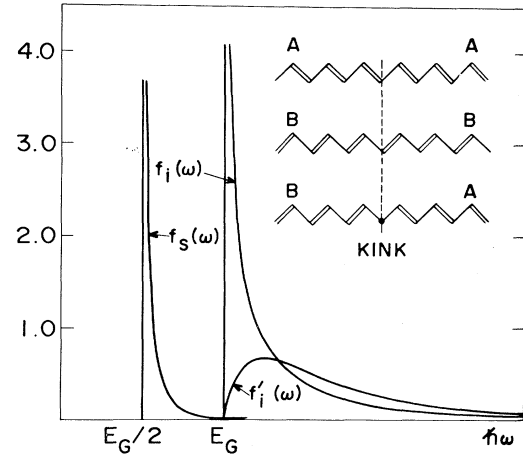


FIG. 1. The absorption functions for a perfect chain [$f_i(\omega)$] and for a chain containing a soliton [$f_s(\omega)$ and $f'_i(\omega)$] are shown. The structure of *trans*-(CH)_x is shown to the right; A phase, B phase, and a chain with a soliton (estimated to extend $\sim 15a$).

$= 4t_0$, m and e are the electron mass and charge, c is the velocity of light, and n is the index of refraction. The energy dependence of $f_i(\omega)$ is shown in Fig. 1. Although $\alpha_i(\omega)$ diverges as $(\hbar\omega - E_g)^{-1/2}$, this square-root singularity will be smeared out by disorder,¹⁴ interchain coupling,¹⁵ or fluctuations.¹⁶

For a *trans*-(CH)_x chain with a static kink [$\Delta(x) = \Delta_0 \tanh(x/\xi)$], the soliton formation energy takes the minimum value $(2/\pi)\Delta_0$ with $\xi = \xi_0 \equiv \hbar v_F / \Delta_0$,¹³ and one bound state appears at midgap. Using the results of Takayama, Lin-Liu, and Maki we calculate α_s , for transitions between a soliton level (S) and the band states, to be

$$\alpha_s(\omega) = A(\pi^2 \xi_0 / a) f_s(\omega), \quad (4)$$

$$f_s(\omega) = \frac{E_g/2}{[(\hbar\omega)^2 - E_g^2/4]^{1/2}} \operatorname{sech}^2 \left(\frac{\pi}{2} \frac{[(\hbar\omega)^2 - E_g^2/4]^{1/2}}{E_g/2} \right). \quad (5)$$

The factor $(\pi^2 \xi_0 / a)$ in Eq. (4) indicates an enhancement of the soliton transition resulting directly from the delocalization of the soliton wave function ($\xi/a \gg 1$). For $W = 10$ eV and $E_g = 1.4$ eV, one finds $\xi_0 \approx 7a$ and $\pi^2 \xi_0 / a \approx 70$. As a result, the transitions involving the soliton level should be observable even at extremely small concentrations. The interband $\alpha'_i(\omega)$ (per carbon atom) in the presence of a kink is

$$\alpha'_i(\omega) = A(\xi_0/L) f'_i(\omega), \quad (6)$$

$$f'_i(\omega) = 16 \frac{\hbar\omega}{\pi E_g} \int \frac{dz}{z' z K' K} \left[\pi \frac{\sinh(\frac{1}{2}\pi K') \cosh(\frac{1}{2}\pi K)}{\cosh(\pi K') - \cosh(\pi K)} - \frac{K'}{K'^2 - K^2} \right]^2, \quad (7)$$

where $z' = (2\hbar\omega/E_g - z)$, $K' = (z'^2 - 1)^{1/2}$, $K = (z^2 - 1)^{1/2}$, and L is the chain length.

The energy dependence of $f_s(\omega)$ and $f'_i(\omega)$ are shown in Fig. 1. The existence of a kink on a chain leads to a strong absorption at midgap due to $\alpha_s(\omega)$, and to the *uniform* suppression of the entire interband transition due to the factor ξ_0/L in Eq. (6).¹⁷

The remarkable change in interband oscillator strength caused by the presence of a soliton can

be understood on a simple physical basis. A perfect dimerized chain has a doubly degenerate ground state, *A* phase and *B* phase (see Fig. 1). Since the soliton is equivalent to a domain wall separating *A* and *B* phases (Fig. 1), the wave functions of the conduction (Ψ_k^c) and valence (Ψ_k^v) bands may be approximated by those of the *A* phase to the right and by those of the *B* phase to the left of the kink. Since the broken symmetry switches the "single and double bonds", $\langle \Psi_k^c(A) | \times p_x | \Psi_k^v(A) \rangle = -\langle \Psi_k^c(B) | p_x | \Psi_k^v(B) \rangle$ and the total matrix element $\langle \Psi_k^c | p_x | \Psi_k^v \rangle$ will vanish. Because of the coherent mixing within the domain wall, the matrix element is nonzero, but reduced by the fractional part of the chain which contributes; i.e., ξ_0/L . In this context, it seems that in Eq. (6), L should not be the full chain length, but the length over which the electronic wave functions are phase coherent; i.e., of the order of the electron mean free path.

The optical absorption spectra of *trans*-(CH)_x are shown in Fig. 2. Curves 1 through 5 on Fig. 2 show the effects of doping: curve 1, undoped; curve 2, very lightly doped with AsF₅ (about 0.01%); curve 3, lightly doped with AsF₅ (about 0.1%); and curve 4, subsequently compensated with NH₃; all data are from the same (CH)_x film. The doping was carried out *in situ* with extreme care so that the results could be directly and quantitatively compared. Curve 5 on Fig. 2 was

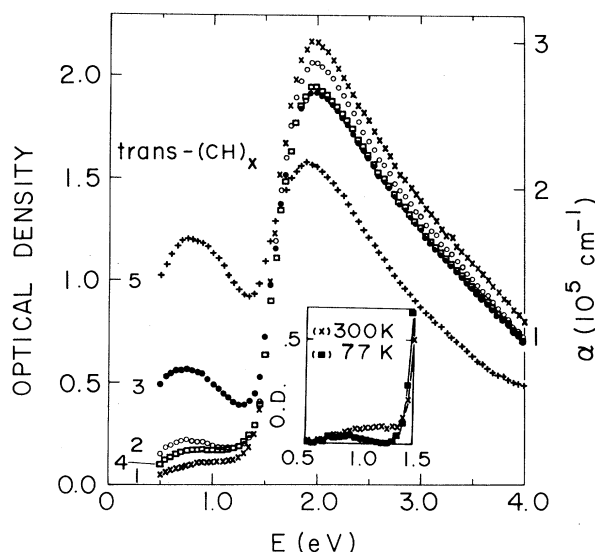


FIG. 2. Absorption spectra of *trans*-(CH)_x: curve 1, undoped; 2, ~0.01% AsF₅; curve 3, ~0.1% AsF₅; curve 4, compensated with NH₃; and curve 5, ~0.5% AsF₅. The inset shows the temperature dependence for undoped *trans*-(CH)_x.

obtained with a separate film doped to a somewhat higher level (~0.5%); quantitative comparison was possible through normalization of the absorption curve prior to doping. The effect of temperature on undoped (CH)_x is shown in the inset; data obtained at 77 and 4.2 K are indistinguishable.

The thin (~1600-Å) (CH)_x films were polymerized¹⁸ at -78 °C on glass substrates and subsequently heated to 200 °C for 2 h to obtain *trans*-(CH)_x. The controlled thickness of the uniform films allowed measurement of more than 2 orders of magnitude change in transmission on the same film. Small base line corrections made by running an identical substrate enabled an accurate measurement in the low- α region. Low-temperature measurements were carried out with use of a Helitran system.

The doping levels are nominal and were estimated from previous experience.⁷ To obtain the 0.01% level, AsF₅ was cooled to $T \approx 90$ K and the stopcock opened into the sample chamber for about one second. This process was then repeated several times to obtain the 0.1% level, etc. The same procedures were followed in earlier experiments⁷ which utilized free-standing films where weight uptake was used to determine the concentration scale.

The strong absorption band with edge at 1.4 eV and peak at 1.95 eV has been attributed¹⁹ to the direct interband transition in a one-dimensional (1D) band structure, and can be viewed as arising from a transition from the 1D peak in the density of states in the valence band to that in the conduction band. The rounding appears to shift the position of the peaks in the VB and CB densities of states by about 0.2 eV. In addition to the main peak, a weak absorption is observed centered near 0.9 eV, corresponding to a transition between the peak in VB density of states and a level inside the gap. Relative to the VB edge, the gap state occurs at about 0.7 eV; i.e., near mid-gap.

On doping with AsF₅, the low-energy absorption grows with increasing concentration and shifts toward lower energy; compensation decreases α almost to the same level as before doping. The strength of the main absorption decreases on doping with AsF₅, but it does not recover after subsequent compensation with NH₃.

The characteristic features of the low-energy and main absorption bands can be explained if we assume that the doping proceeds through formation of positive charged solitons (S^+) and that the

low-energy α is associated with the transition from the valence band into the S^+ level to form a neutral soliton (S^0). The low-energy absorption, seen in the low-temperature data of inset to Fig. 2, indicates that soliton states are also present in the undoped material. As the number of S^+ increases with AsF_5 doping, the strength of the low-energy transition ($S^+ + e \rightarrow S^0$) grows proportionally. Further, the calculations presented above predict that the interband transition will be suppressed with the introduction of soliton kinks, again in qualitative agreement with the experimental results. On reacting with NH_3 , the S^+ level is compensated, and the low-energy band decreases accordingly. On the other hand, the interband transition does not recover to its initial strength on compensation, since the π -electron kinks remain on the chain; only the charged center is compensated.

The integrated intensity of the low-energy absorption band after $\sim 0.1\%$ doping (curve 3) is about one-tenth of that of the main absorption band of the undoped sample. We infer from Eq. (4) a value for $\pi^2 \xi_0 / a \sim 10^2$ in good agreement with the theoretical value. The *uniform* decrease in intensity of the interband transition is also evident in curve 3 and corresponds to about a 10% reduction relative to the undoped sample. Assuming soliton doping, we have about one per 10^3 carbon atoms implying that each kink removes about 10^2 carbon atoms from the interband transition, in general agreement with Eq. (6).

The data indicate a gap state about 0.7 eV above the VB edge; i.e., at the center of the 1.4-eV gap. This is consistent with recent studies¹¹ which showed that the enhanced photoconductivity in *trans*-(CH)_x is directly related to the presence of localized states generated by isomerization and/or doping with energy near midgap.

Alternative explanations must be considered including the analog of conventional doping⁷ and the formation of metallic islands.¹² The large effects observed at such low concentrations are difficult to explain. For example, if one assumes high-concentration metallic island formation at these low levels, then more than 99% of the sample would be unaffected, implying no change in the interband transition. Experiments⁷ with other dopants indicate that the properties are independent of the dopant size, charge, etc., in contrast to the detailed changes expected for conventional doping. Finally, the uniform suppression of the entire interband transition, the concentration dependence of the low-energy α on doping, and the

onset of photoconductivity near midgap¹¹ rule out the possibility of exciton formation.

Within this simple single-particle picture, compensation would convert S^+ to S^0 , suggesting that the transition to the conduction band ($S^0 \rightarrow S^+ + e$) would dominate. This is not observed, implying that the compensation is more complicated, perhaps involving a chemical reaction with the S^+ carbonium ion to form a neutral covalent complex.

In conclusion, calculations within the soliton model lead to two specific predictions: (1) The intensity of transitions involving the soliton level should be enhanced by about 2 orders of magnitude. (2) The existence of a soliton domain wall on a chain suppresses the interband transition. Both of these effects are observed experimentally with magnitudes in approximate agreement with the theoretical results.

We are grateful to Professor J. R. Schrieffer for important comments. We thank Dr. S. Kivelson for useful discussions. Dr. Suzuki acknowledges support from the Yamada Science Foundation. This research was supported by the U. S. Office of Naval Research.

^(a)On leave from Faculty of Engineering Science, Osaka University, Osaka, Japan.

^(b)Permanent address: Asahi Chemical Industry Co., Ltd., 2-1 Samejima, Fuji-shi 1416, Shizuoka-ken, Japan.

¹W. P. Su, J. R. Schrieffer, and A. J. Heeger, Phys. Rev. Lett. **42**, 1698 (1979), and Phys. Rev. B **22**, 2099 (1980).

²M. J. Rice, Phys. Lett. **71A**, 152 (1979).

³I. B. Goldberg, H. R. Crowe, P. R. Newman, A. J. Heeger, and A. G. MacDiarmid, J. Chem. Phys. **70**, 1132 (1979).

⁴B. R. Weinberger, J. Kaufer, A. Pron, A. J. Heeger, and A. G. MacDiarmid, Phys. Rev. B **20**, 223 (1979).

⁵M. Nechtschein, F. Devreux, R. L. Greene, T. C. Clarke, and G. B. Street, Phys. Rev. Lett. **44**, 356 (1980).

⁶B. R. Weinberger, E. Ehrenfreund, A. Pron, A. J. Heeger, and A. G. MacDiarmid, J. Chem. Phys. (to be published).

⁷C. R. Fincher, Jr., M. Ozaki, A. J. Heeger, and A. G. MacDiarmid, Phys. Rev. B **19**, 4140 (1979).

⁸E. J. Mele and M. J. Rice, Phys. Rev. Lett. **45**, 926 (1980).

⁹Y. W. Park, A. Denenstein, C. K. Chiang, A. J. Heeger, and A. G. MacDiarmid, Solid State Commun. **29**, 747 (1979).

¹⁰Y. W. Park, A. J. Heeger, M. A. Druy, and A. G. MacDiarmid, J. Chem. Phys. **73**, 946 (1980).

¹¹S. Etemad, M. Ozaki, D. L. Peebles, A. J. Heeger,

and A. G. MacDiarmid, to be published.

¹²Y. Tomkiewicz, T. D. Schultz, H. B. Brown, T. C. Clarke, and G. B. Street, Phys. Rev. Lett. **43**, 1532 (1979).

¹³H. Takayama, Y. R. Lin-Liu, and K. Maki, Phys. Rev. B **21**, 2388 (1980).

¹⁴D. Vanderbilt and E. J. Mele, Phys. Rev. B (to be published).

¹⁵P. M. Grant and I. P. Batra, Solid State Commun. **29**, 225 (1978).

¹⁶S. A. Brazovskii, Pis'ma Zh. Eksp. Teor. Fiz. **28**, 606 (1978) [JETP Lett. **28**, 656 (1978)].

¹⁷The suppression of the interband transition [Eq. (6)] and the associated decrease in total oscillator strength have been calculated here within the continuum model (Ref. 13). Theoretical studies of the more realistic discrete lattice are underway using the model of Su, Schrieffer, and Heeger.

¹⁸T. Ito, H. Shirakawa, and S. Ieda, J. Polym. Sci., Polym. Chem. Ed. **13**, 1943 (1975), and references therein.

¹⁹C. R. Fincher, Jr., M. Ozaki, M. Tanaka, D. Peebles, L. Lauchlan, A. J. Heeger, and A. G. MacDiarmid, Phys. Rev. B **20**, 1589 (1979).

Possible Mechanism of Superconductivity in Metal-Semiconductor Eutectic Alloys

C. S. Ting and D. N. Talwar

Department of Physics, University of Houston, Houston, Texas 77004

and

K. L. Ngai

Naval Research Laboratory, Washington, D. C. 20375

(Received 6 May 1980)

The effect due to the tunneling of conduction electrons into the negative- U centers at the disordered metal-semiconductor interfaces on the superconductivity of metal-semiconductor eutectic alloys is considered. Gorkov's formalism is used to calculate T_c for (i) $n_I \ll 1$ and $\lambda \neq 0$, (ii) $\lambda = 0$. Where n_I is the concentration of the pairing centers and λ is the phonon-mediated electron-electron interaction in BCS theory. Our results can qualitatively explain the increase of T_c in Al-Si, Al-Ge, and Be-Si eutectic alloys.

PACS numbers: 74.10.+v, 73.40.Ns

Recently, there has been some interest in the study of superconductivity in metal-semiconductor mixture systems both experimentally¹⁻³ and theoretically.^{4,5} Substantial enhancement of the superconducting transition temperatures T_c have been observed for Al-Ge, Al-Si and Be-Si eutectic alloys.^{1,2} However, no increase of T_c has been found for thin Al films grown epitaxially on Si substrates.³ The observed enhancement of T_c (Ref. 2) was attributed to the exciton mechanism

of Allender *et al.*⁴ More recently, Simanek⁵ suggested that the disordered interfaces are essential for the enhancement of T_c . The ideas of Anderson⁶ and Varma and Pandey,⁷ who proposed that metal-semiconductor bonds at a disordered interface exhibit a net negative correlation energy due to the bipolaron interaction, have been employed to study the superconductivity for various kinds of systems.^{5,8} The effective Hamiltonian can be written as

$$H = H_{\text{BCS}} + \sum_{k,\alpha} \epsilon_k a_{k\alpha}^\dagger a_{k\alpha} + \sum_{j,\alpha} E_d b_{j\alpha}^\dagger b_{j\alpha} + \sum_j \sum_{k,\alpha} [v_{kd} a_{k\alpha}^\dagger b_{j\alpha} \exp(i\vec{k} \cdot \vec{R}_j) + \text{H.c.}] + U \sum_j n_{j\uparrow} n_{j\downarrow}, \quad (1)$$

where H_{BCS} is the BCS Hamiltonian which describes the phonon-mediated electron-electron interaction.⁹ $a_{k\alpha}^\dagger$ ($a_{k\alpha}$) is the creation (annihilation) operator for conduction electrons with energy ϵ_k and spin α in the metallic matrix $n_{j\alpha} = b_{j\alpha}^\dagger b_{j\alpha}$ and $b_{j\alpha}^\dagger$ ($b_{j\alpha}$) is the corresponding operator for the localized electron at the covalent bond of the metal-semiconductor interface at site j . E_d is the energy level of the localized electron measured from the Fermi energy.

The above equation is a simplification of the original Hamiltonian^{7,8} which involves electron-local-phonon interaction g and the local-phonon frequency ω_c . The "s-d" tunneling matrix element v_{kd} is substantially reduced from its value in the original Hamiltonian by the orthogonality blocking (phonon overlap). The effective interaction U between the localized electrons can be attractive ($U < 0$) if the value of ω_c is high. We